

# Size-dependent vibration of nickel cantilever microbeams: Experiment and gradient elasticity

Cite as: AIP Advances 6, 105202 (2016); <https://doi.org/10.1063/1.4964660>

Submitted: 13 August 2016 • Accepted: 27 September 2016 • Published Online: 05 October 2016

Jian Lei, Yuming He, Song Guo, et al.



View Online



Export Citation



CrossMark

## ARTICLES YOU MAY BE INTERESTED IN

[On differential equations of nonlocal elasticity and solutions of screw dislocation and surface waves](#)

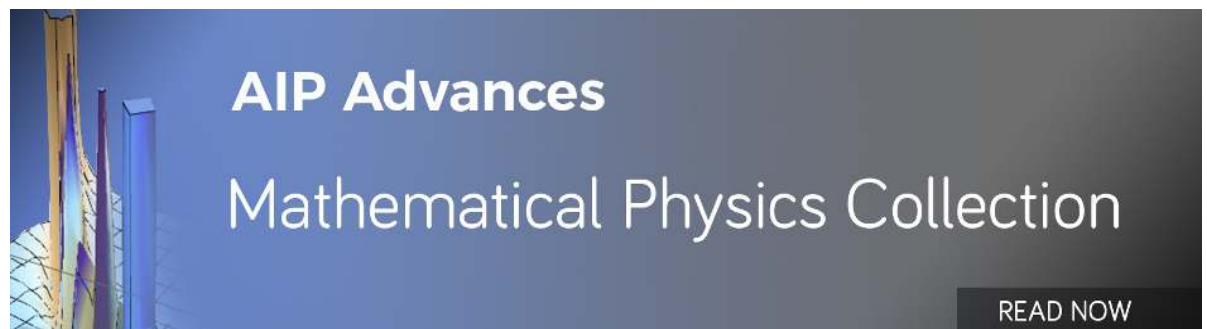
Journal of Applied Physics **54**, 4703 (1983); <https://doi.org/10.1063/1.332803>

[Nonlocal continuum theories of beams for the analysis of carbon nanotubes](#)

Journal of Applied Physics **103**, 023511 (2008); <https://doi.org/10.1063/1.2833431>

[Column buckling of multiwalled carbon nanotubes using nonlocal continuum mechanics](#)

Journal of Applied Physics **94**, 7281 (2003); <https://doi.org/10.1063/1.1625437>



AIP Advances  
Mathematical Physics Collection

READ NOW

## Size-dependent vibration of nickel cantilever microbeams: Experiment and gradient elasticity

Jian Lei,<sup>1,2</sup> Yuming He,<sup>1,2,a</sup> Song Guo,<sup>1,2</sup> Zhenkun Li,<sup>1,2</sup> and Dabiao Liu<sup>1,2</sup>

<sup>1</sup>Department of Mechanics, Huazhong University of Science and Technology, Wuhan 430074, China

<sup>2</sup>Hubei Key Laboratory of Engineering Structural Analysis and Safety Assessment, Wuhan 430074, China

(Received 13 August 2016; accepted 27 September 2016; published online 5 October 2016)

The size-dependent elasticity of a series of nickel cantilever microbeams was investigated experimentally for the first time. The experimental results revealed that the dimensionless natural frequencies of the cantilever microbeams increase to about 2.1 times with the beam thickness decreasing from 15 to 2.1  $\mu\text{m}$ . Furthermore, based on the strain gradient elasticity theory (SGT) and by using the differential quadrature method (DQM) and the least square method (LSM), the experimental results were interpreted and the material length scale parameters in the scale of micron in elastic range were obtained. This investigation will be useful and helpful for the theoretical and numerical simulation of micro-structures and important for the design of the MEMS/NEMS. © 2016 Author(s). All article content, except where otherwise noted, is licensed under a Creative Commons Attribution (CC BY) license (<http://creativecommons.org/licenses/by/4.0/>). [<http://dx.doi.org/10.1063/1.4964660>]

### I. INTRODUCTION

Microbeams and microplates are the main components of micro- and nano-electro mechanical systems (MEMS and NEMS), such as micro-resonators,<sup>1</sup> Atomic Force Microscopes (AFMs),<sup>2</sup> micro-switches<sup>3</sup> and micro-actuators,<sup>4</sup> etc. Many experiments, mainly about the plastic behaviors, have found that the mechanical behaviors of the micro- and nano-structures are size-dependent when the characteristic dimension of the structures is in the micro- and nano-meter scale.<sup>5–18</sup> For example, Fleck et al.<sup>9</sup> found that the normalized torque increases dramatically with the wire diameter decreasing from 170 to 20  $\mu\text{m}$  in the torsion tests of polycrystalline copper wires. Liu et al.<sup>10</sup> also observed the significant size effects at initial yielding and plastic flow stress in the torsion test of polycrystalline copper wires with diameters from 18 to 105  $\mu\text{m}$ . In addition, experiments on the size-dependent elasticity of the micro-structures in the scale of nano-meter can be found in open literature.<sup>19,20</sup> For instance, Shin et al.<sup>20</sup> found the elastic modulus of a single EAP nanofiber is size-dependent with the diameter from 50 to 110 nm due to the influence of the surface effect. However, at micro-meter scale, the experiments on size-dependent elasticity are very limited.<sup>21,22</sup> Lam et al.<sup>21</sup> performed the micro bending test of epoxy beams, and found that the normalized bending rigidity increases about 2.4 times as the thickness of the microbeam reduces from 115 to 20  $\mu\text{m}$  due to the effect of strain gradient elasticity. It should be pointed that the experimental reports on size-dependent elasticity in the scale of micron mainly focused on the micro-structures composed of non-metallic materials, and the experimental method was static bending test by using the AFM.

The classical continuum theory is size-independent and cannot predict the small-scale effects. Thus, for capturing the size effects of micro and nano-structures, various higher-order continuum theories involving additional material length scale parameters have been proposed. For example, the classical couple stress theory,<sup>23,24</sup> nonlocal elasticity theory,<sup>25</sup> surface elasticity theory,<sup>26,27</sup> strain

<sup>a</sup>Corresponding author. E-mail: [ymhe01@sina.com](mailto:ymhe01@sina.com)



gradient theory,<sup>9,21</sup> modified couple stress theory<sup>28</sup> and nonlocal strain gradient theory.<sup>29</sup> Based on these theories, theoretical and numerical investigations on small-scale effects of micro-structures have been performed.<sup>30–39</sup>

Review of the previous research on the size effects of the micro-structures in the scale of micron, most of the investigations are the theoretical and numerical simulation, however, the experimental investigations of size effects and the measurement of the material length scale parameters in elastic range are very limited, especially on size-dependent elasticity of metal micro-scale structures. In this study, an experimental study of size-dependent elasticity for cantilever microbeams composed of nickel by using a dynamic test was reported for the first time.

## II. EXPERIMENT DESIGN

The nickel foils (99.99% purity) with thicknesses ( $h$ ) of 2.1, 3.2, 5.2, 10.0 and 15.0  $\mu\text{m}$  (with the thickness tolerance of 0.2  $\mu\text{m}$ ) were employed in this study. The Young's modulus ( $E$ ) and the mass density ( $\rho$ ) of nickel are 207 GPa and 8900  $\text{kg}/\text{m}^3$ , respectively. Each foil was cut into 5 strips with 1 mm wide and 17 mm long (shown in FIG. 1(a)) with the length tolerance of 0.15 mm for reducing the errors of the experiment by multiple independent measurements. Then these stripes were vacuum annealed at 300°C for 5 hours to eliminate the machining residual stresses. A cantilever microbeam with width 1 mm and length 5 mm was obtained by clamping a strip to a special gripper (the deepness of the gripper is 12 mm), as shown in FIG. 1(b). Furthermore, the typical images of the surface morphology and the roughness of the foils were measured by using the laser microscope, as shown in FIG. 1(c) and (d). From the Figure, the roughness is very small (less than 2 percent of the thickness of the foils) and the surface smoothness is enough for our experimental study (the roughness of the foils with 2.1, 10.0 and 15.0  $\mu\text{m}$  thickness is 0.036, 0.028 and 0.039  $\mu\text{m}$  respectively which are not given in FIG. 1).

A vibration test system made up of laser Doppler vibrometer (LDV), PC, loudspeaker and three-dimensional translation stage was used to measure the natural frequencies of the nickel cantilever microbeams, as shown in FIG. 2(a). During the test process, a nickel cantilever microbeam was fixed on the top surface of the three-dimensional translation stage. The sinusoidal sound signal was produced by the loudspeaker to act upon the cantilever microbeam. The real-time vibration responses of the cantilever microbeam were captured by the LDV and displayed on the PC. To obtain the natural frequency of the cantilever microbeam, the frequency of the sinusoidal sound signal was modulated in a certain frequency range with the accuracy of 0.1 Hz. While the resonant response of the cantilever microbeam was captured by the LDV, one can obtain the natural frequency of the cantilever microbeam which was equal to the resonant frequency.

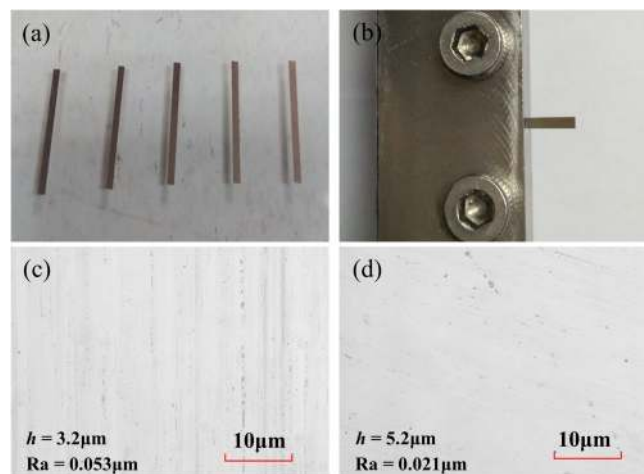


FIG. 1. Typical images of the: (a) nickel stripes; (b) nickel cantilever microbeam; (c) and (d): surface morphology and the roughness of the foils.

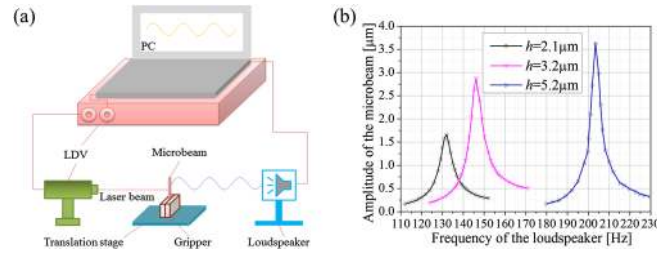


FIG. 2. (a) A schematic of the vibration test system; (b) Typical frequency–response curves of the cantilever microbeams.

TABLE I. Natural frequencies of the cantilever microbeams with different thickness.

Thickness ( $\mu\text{m}$ )	Natural frequency of experimental values (Hz)					Mean value (Hz)
	1	2	3	4	5	
2.1	118.9	132.2	136.5	140.3	153.9	136.4
3.2	138.1	141.0	145.9	148.3	162.2	147.1
5.2	202.3	204.7	209.0	211.9	212.9	208.2
10.0	347.6	352.5	371.6	381.2	390.0	368.6
15.0	440.7	448.9	449.9	457.2	465.7	452.5

Repeating the above test, the natural frequency of each cantilever microbeam was obtained in TABLE 1. In addition, the typical frequency-response curves of the cantilever microbeams (2.1, 3.2 and 5.2  $\mu\text{m}$  thickness) were given in FIG. 2(b), from the figure, the resonant responses were observed and the natural frequencies of the microbeams could be obtained directly.

### III. RESULTS AND DISCUSSION: STRAIN GRADIENT ELASTICITY

In order to analyze the experimental results, the following process was performed. Based on the classical Bernoulli-Euler beam theory, the analytical solution of the classical natural frequency of a cantilever beam is given by

$$\omega_{ct} = \frac{(s_n L)^2}{2\pi} \sqrt{\frac{EI}{\rho b h L^4}}, \quad s_n L = 1.875, 4.694, 7.855 \quad (1)$$

where  $EI$  is the bending rigidity of the microbeam,  $h$  is the thickness,  $b$  is the width,  $L$  is the length,  $n$  is the order of the frequency, and  $I = bh^3/12$ . In this experiment, the obtained natural frequencies of the nickel cantilever microbeams were the first-order natural frequency, thus the value of  $s_n L$  is set to 1.875.

The dimensionless frequency (frequency ratio) is defined as

$$\hat{\omega} = \omega / \omega_{ct} \quad (2)$$

where  $\omega$  is the obtained natural frequency of the nickel cantilever microbeams.

The dimensionless bending rigidity (the ratio of bending rigidity) can be given as

$$\xi = (\omega / \omega_{ct})^2 \quad (3)$$

Then one can obtain the dimensionless frequency and the dimensionless bending rigidity based on TABLE 1, Eqs. (1), (2) and (3), as shown in FIG. 3.

From FIG. 3, one can observe that the dimensionless frequency increases to about 2.1 times and the dimensionless bending rigidity increases to about 4.4 times with decreasing the beam thickness from 15 to 2.1  $\mu\text{m}$ . It reveals that the elastic vibration of the nickel cantilever microbeams is size-dependent in the scale of micron, which was not reported in other open literature.

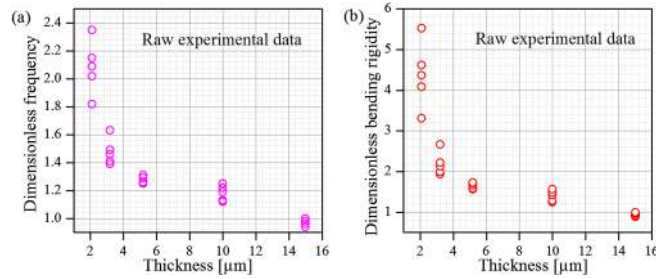


FIG. 3. Raw experimental data for: (a) dimensionless frequency; (b) dimensionless bending rigidity.

In order to capture the size effects of the micro-structures, Lam et al.<sup>21</sup> developed the strain gradient elasticity theory (SGT) which involves three material length scale parameters corresponding to the dilatation gradient vector, the deviatoric stretch gradient tensor and the curvature tensor respectively. Based on the SGT and the variational principle, Kong et al.<sup>33</sup> and Kahrobaian et al.<sup>40</sup> gave the equation of motion of the microbeams as

$$S \frac{\partial^4 w}{\partial x^4} - K \frac{\partial^6 w}{\partial x^6} + \rho A \frac{\partial^2 w}{\partial t^2} = 0 \quad (4)$$

where

$$K = I \left( 2\mu l_0^2 + \frac{4}{5} \mu l_1^2 \right), \quad S = EI + 2\mu A l_0^2 + \frac{8}{15} \mu A l_1^2 + \mu A l_2^2 \quad (5)$$

and  $l_0$ ,  $l_1$  and  $l_2$  are additional material length scale associated with dilatation gradient, deviatoric stretch gradient and rotation gradient, respectively, and  $A = bh$ .

For cantilever microbeams, the differential quadrature method (DQM) is employed to solve the partial differential equation for obtaining the natural frequency. Based on the DQM, the beam domain is discretized by  $N$  nodes along the neutral axis ( $x$ -axis), the value of  $w$  and its partial derivative with respect to  $x$  can be approximated by

$$w = \sum_{i=1}^N l_i(\xi) w_i, \quad \left. \frac{\partial^m w}{\partial \xi^m} \right|_{\xi=\xi_i} = \sum_{j=1}^N C_{ij}^{(m)} w_j \quad (6)$$

where  $l_i(\xi)$  is Lagrange interpolation polynomial and  $C_{ij}^{(m)}$  is the weighting coefficients whose recursive formula can be found in literature.<sup>41,42</sup> The sample points are selected to be the Chebyshev-Gauss-Lobatto points as<sup>43</sup>

$$\begin{aligned} \xi_1 = 0, \quad \xi_2 = 0.0001L, \quad \xi_{N-1} = 0.9999L, \quad \xi_N = L, \\ \xi_i = \frac{L}{2} \left( 1 - \cos \left( \frac{(i-2)\pi}{N-3} \right) \right), \quad i = 3, \dots, N-2 \end{aligned} \quad (7)$$

By employing the DQM, the discrete counterpart of the equation of motion can be derived as

$$S \sum_{j=1}^N C_{ij}^{(4)} w_j - K \sum_{j=1}^N C_{ij}^{(6)} w_j + \rho A \frac{\partial^2 w}{\partial t^2} = 0 \quad (8)$$

The associated boundary conditions of the cantilever microbeam can be given as

$$w_i = 0, \quad \sum_{j=1}^N C_{ij}^{(1)} w_j = 0, \quad i = 1,$$

$$\sum_{j=1}^N C_{ij}^{(2)} w_j = 0, \quad \sum_{j=1}^N C_{ij}^{(3)} w_j = 0, \quad i = N \quad (9)$$

By denoting the unknown displacement vector as following

$$\mathbf{d} = \{u_i\}, i = 1, 2, \dots, N \quad (10)$$

Based on the Eqs. (8) and (9), we have the following matrix form

$$\mathbf{K}\mathbf{d} + \mathbf{M}\ddot{\mathbf{d}} = 0 \quad (11)$$

where  $\mathbf{K}$  is the stiffness matrix;  $\mathbf{M}$  is the mass matrix.

Expand the displacement vector  $\mathbf{d}$  in the form of

$$\mathbf{d} = \mathbf{d}^* e^{i\omega t} \quad (12)$$

where  $\mathbf{d}^* = \{u_i^*\}$  is the vibration mode shape vector. Then we can obtain the eigenvalue equation as

$$\mathbf{K}\mathbf{d}^* - \omega^2 \mathbf{M}\mathbf{d}^* = 0 \quad (13)$$

By solving the Eq. (13), the natural frequency of the cantilever microbeams can be obtained.

For obtaining the values of the material length scale parameters ( $l_0$ ,  $l_1$  and  $l_2$ ), the method of minimization of least squares of the error between the experimental results (TABLE 1) and the SGT results (solved by Eq. (13)) was employed. In the process of calculation, the values of the three material length scale parameters are set to equal to each other ( $l_0 = l_1 = l_2 = l$ ),<sup>22,33</sup> the resolution of the  $l$  is defined as  $\Delta l = 1$  nm, the sample points  $N$  is set to 20 which can give convergent results. Then the value of the material length scale parameters of nickel microbeams for SGT can be obtained as  $l_0 = l_1 = l_2 = l = 0.843$   $\mu\text{m}$ . It should be noted that by setting  $l_0 = l_1 = 0$ , the SGT can be reduced to the modified couple stress theory (MCST),<sup>28</sup> thus by using the solving process above, one can obtain the value of the material length scale of nickel microbeams for MCST as  $l_2 = l = 1.553$   $\mu\text{m}$ . Compared to the value of the material length scale of epoxy microbeams (the value for SGT is 11.01  $\mu\text{m}$ ,<sup>21,40</sup> for MCST is 17.6  $\mu\text{m}$ <sup>21,35</sup>), the value of the material length scale of nickel microbeam is smaller than one-tenth of that of epoxy microbeam, it reveals that the material length scale parameters have important relationship with the material's micro-structure.

By using the material length scale of nickel microbeams for SGT and MCST, the dimensionless frequency based on the SGT ( $l = 0.843$   $\mu\text{m}$ ), MCST ( $l = 1.553$   $\mu\text{m}$ ), classical theory ( $l = 0$ ) and the mean values of experimental results are displayed in FIG. 4. From FIG. 4, it can be seen that the experimental results agree well with those predicted by the SGT and the MCST. Meanwhile, the SGT and the MCST give nearly the same results, however, the value of the material length scale is very different as the MCST ignores the influences of the dilatation gradient and the deviatoric stretch gradient.

For investigating the influences of different gradient elasticity on dimensionless natural frequencies of cantilever microbeams, the results which only consider the dilatation gradient (by setting  $l_0 = 0.843$   $\mu\text{m}$  and  $l_1 = l_2 = 0$ ), deviatoric stretch gradient (by setting  $l_1 = 0.843$   $\mu\text{m}$  and  $l_0 = l_2 = 0$ )

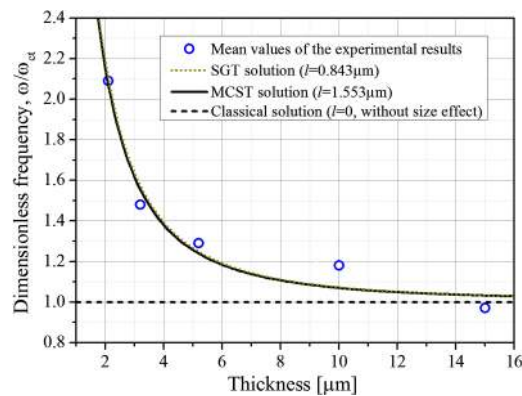


FIG. 4. Mean values of the experimental results, SGT solution, MCST solution and the classical solution of the dimensionless natural frequencies for the nickel cantilever microbeams.

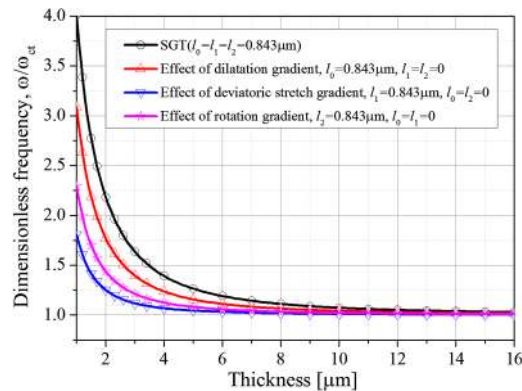


FIG. 5. The effects of dilatation gradient, deviatoric stretch gradient and rotation gradient on dimensionless natural frequencies of cantilever microbeams.

and rotation gradient (by setting  $l_2 = 0.843 \mu\text{m}$  and  $l_0 = l_1 = 0$ ) are presented respectively in FIG. 5. From the Figure, one can observed that for the SGT microbeam model, the dilatation gradient has the greatest influence on the microbeams, then is the rotation gradient, and the deviatoric stretch gradient has the least influence.

#### IV. CONCLUSIONS

In conclusion, an experimental study of elastic vibration for nickel cantilever microbeams was performed in this paper. The experimental results revealed that the dimensionless natural frequency and dimensionless bending rigidity of nickel cantilever microbeams increase with decreasing the beam thickness. It indicates the size-dependent elasticity of metal (nickel) microbeams by experiment for the first time. Furthermore, in the light of the SGT and by using the DQM and the least square method, the experimental results were interpreted and the material length scale parameters in the scale of micron in elastic range were obtained. For comparison, the value of material length scale parameter for MCST is given as well. As the MCST ignores the influences of the dilatation gradient and the deviatoric stretch gradient, the value of material length scale parameter is larger than that for SGT. In addition, compared to the value of the material length scale of epoxy microbeams, the value of the material length scale of nickel microbeam is smaller than one-tenth of that of epoxy microbeam, it reveals that the material length scale parameters have important relationship with the material's micro-structure. The results will be useful and helpful for the theoretical and numerical simulation of micro-structures and the design of the MEMS.

#### ACKNOWLEDGMENTS

This work was financially supported by the National Natural Science Foundation of China (Nos.11272131, 11472114), the Natural Science Foundation of Hubei Province (No. 2015CFB394), and the Fundamental Research Funds for the Central Universities, HUST: no. 2015QN138.

- <sup>1</sup> J. Zook, D. Burns, H. Guckel, J. Sniegowski, R. Engelstad, and Z. Feng, *Sensors and Actuators A: Physical* **35**(1), 51–59 (1992).
- <sup>2</sup> A. Torii, M. Sasaki, K. Hane, and S. Okuma, *Sensors and Actuators A: Physical* **44**(2), 153–158 (1994).
- <sup>3</sup> D. Acquaviva, A. Arun, R. Smajda, D. Grogg, A. Magrez, T. Skotnicki, and A. Ionescu, *Procedia Chemistry* **1**(1), 1411–1414 (2009).
- <sup>4</sup> E. S. Hung and S. D. Senturia, *Journal of Microelectromechanical Systems* **8**(4), 497–505 (1999).
- <sup>5</sup> J.-Y. Kim, D. Jang, and J. R. Greer, *Scripta Mater* **61**(3), 300–303 (2009).
- <sup>6</sup> A. T. Jennings, M. J. Burek, and J. R. Greer, *Phys Rev Lett* **104**(13), 135503 (2010).
- <sup>7</sup> D. Dunstan, B. Ehrler, R. Bossis, S. Joly, K. P'ng, and A. Bushby, *Phys Rev Lett* **103**(15), 155501 (2009).
- <sup>8</sup> J. S. Stölken and A. G. Evans, *Acta Mater* **46**(14), 5109–5115 (1998).
- <sup>9</sup> N. A. Fleck, G. M. Muller, M. F. Ashby, and J. W. Hutchinson, *AcM&M* **42**(2), 475–487 (1994).
- <sup>10</sup> D. Liu, Y. He, X. Tang, H. Ding, P. Hu, and P. Cao, *Scripta Mater* **66**(6), 406–409 (2012).
- <sup>11</sup> D. Liu, Y. He, D. Dunstan, B. Zhang, Z. Gan, P. Hu, and H. Ding, *Phys Rev Lett* **110**(24), 244301 (2013).



- <sup>12</sup> Q. Yu, L. Qi, R. K. Mishra, X. Zeng, and A. M. Minor, *Appl Phys Lett* **106**(26), 261903 (2015).
- <sup>13</sup> Y.-J. Wang, G.-J. J. Gao, and S. Ogata, *Appl Phys Lett* **102**(4), 041902 (2013).
- <sup>14</sup> Z. Gan, Y. He, D. Liu, B. Zhang, and L. Shen, *Scripta Mater* **87**, 41–44 (2014).
- <sup>15</sup> H. Zbib and E. Aifantis, *Scripta Mater* **48**(2), 155–160 (2003).
- <sup>16</sup> P. Gu and M. Dao, *Appl Phys Lett* **102**(9), 091904 (2013).
- <sup>17</sup> J.-Y. Kim and J. R. Greer, *Appl Phys Lett* **93**(10), 101916 (2008).
- <sup>18</sup> C. Deng and F. Sansoz, *Appl Phys Lett* **95**(9), 091914 (2009).
- <sup>19</sup> R. Lakes, *Int J Solids Struct* **22**(1), 55–63 (1986).
- <sup>20</sup> M. K. Shin, S. I. Kim, S. J. Kim, S.-K. Kim, H. Lee, and G. M. Spinks, *Appl Phys Lett* **89**(23), 231929 (2006).
- <sup>21</sup> D. C. C. Lam, F. Yang, A. C. M. Chong, J. Wang, and P. Tong, *J Mech Phys Solids* **51**(8), 1477–1508 (2003).
- <sup>22</sup> C. Liebold and W. H. Müller, *Comp Mater Sci* (2015).
- <sup>23</sup> R. A. Toupin, *Arch Ration Mech An* **11**(1), 385–414 (1962).
- <sup>24</sup> R. D. Mindlin and H. F. Tiersten, *Arch Ration Mech An* **11**(1), 415–448 (1962).
- <sup>25</sup> A. C. Eringen, *Int J Eng Sci* **10**(1), 1–16 (1972).
- <sup>26</sup> M. E. Gurtin and A. I. Murdoch, *Arch Ration Mech An* **57**(4), 291–323 (1975).
- <sup>27</sup> M. E. Gurtin and A. I. Murdoch, *Int J Solids Struct* **14**(6), 431–440 (1978).
- <sup>28</sup> F. Yang, A. C. M. Chong, D. C. C. Lam, and P. Tong, *Int J Solids Struct* **39**(10), 2731–2743 (2002).
- <sup>29</sup> C. Lim, G. Zhang, and J. Reddy, *J Mech Phys Solids* **78**, 298–313 (2015).
- <sup>30</sup> R. Ansari, R. Gholami, and S. Sahmani, *Compos Struct* **94**(1), 221–228 (2011).
- <sup>31</sup> J. Lei, Y. He, B. Zhang, Z. Gan, and P. Zeng, *Int J Eng Sci* **72**, 36–52 (2013).
- <sup>32</sup> B. Zhang, Y. He, D. Liu, J. Lei, L. Shen, and L. Wang, *Composites Part B: Engineering* (2015).
- <sup>33</sup> S. Kong, S. Zhou, Z. Nie, and K. Wang, *Int J Eng Sci* **47**(4), 487–498 (2009).
- <sup>34</sup> L.-L. Ke, J. Yang, S. Kitipornchai, and Y.-S. Wang, *Int J Eng Sci* **81**, 66–81 (2014).
- <sup>35</sup> S. Park and X. Gao, *J Micromech Microeng* **16**(11), 2355 (2006).
- <sup>36</sup> L. Wang, W.-B. Liu, and H.-L. Dai, *Physica E: Low-dimensional Systems and Nanostructures* **66**, 87–92 (2015).
- <sup>37</sup> J. Lei, Y. He, B. Zhang, D. Liu, L. Shen, and S. Guo, *Int J Mech Sci* **104**, 8–23 (2015).
- <sup>38</sup> J. Reddy, *J Mech Phys Solids* **59**(11), 2382–2399 (2011).
- <sup>39</sup> B. Akgöz and Ö. Civalek, *Int J Mech Sci* **99**, 10–20 (2015).
- <sup>40</sup> M. Kahrobaiyan, M. Asghari, and M. Ahmadian, *Finite Elem Anal Des* **68**, 63–75 (2013).
- <sup>41</sup> R. Ansari, R. Gholami, M. F. Shojaei, V. Mohammadi, and S. Sahmani, *European Journal of Mechanics-A/Solids* **49**, 251–267 (2015).
- <sup>42</sup> S. Sahmani, M. Bahrami, and R. Ansari, *Compos Struct* **110**, 219–230 (2014).
- <sup>43</sup> C. W. Bert and M. Malik, *ApMRv* **49**(1), 1–28 (1996).